

**LOCOMOTION AND VESTIBULAR OCULAR MOTOR  
CONTROL**

NETTA GURARI  
ADVISORS: PROFESSOR VIJAY KUMAR  
DR. DAVID SOLOMON

[c!]

---

*Date:* December 19, 2003.

CONTENTS

List of Figures	2
1. Abstract	3
2. Introduction	3
3. Background	4
3.1. Motion Control	4
3.2. Mathematical Theory	7
4. Experimental Setup and Procedures	12
4.1. OPTOTRAK and Force Plate	12
4.2. Torsion Pendulum	13
5. Results	15
5.1. OPTOTRAK and Force Plates	15
5.2. Torsion Pendulum	19
5.3. Simulation	19
6. Discussion	20
7. Conclusions and Future Work	22
8. Acknowledgements	23
References	23

LIST OF FIGURES

1 Postural Control	5
2 Stabilization, En bloc, and Head-on-Body Techniques	7
3 One Legged Model	8
4 Mathematical Model	9
5 OPTOTRAK and Force Plate	12
6 The Linear Pendulum Apparatus	14
7 Torsion Pendulum	15
8 Position with respect to time	16
9 Joint segments with respect to time	16
10 General features of pivot turn	17
11 Torque applied to ground	17
12 B and K Values	18
13 Simulated pivot turn at an initial time	20
14 Simulated pivot turn at a middle time	20

## 1. ABSTRACT

For my senior project, I have created a new human model to analyze a pivot turn. A right pivot turn is designated as a clockwise turn with the left leg planted on the ground and the right leg swinging (the motion of the leg rotating away from the center of axis and then back to the initial stance of the legs together). This model describes the human body as a three-segment system with three joints.  $I_1$  (I=moment of inertia) is the leg in contact with the ground,  $I_2$  is the trunk section including the leg held out to the side, and  $I_3$  is the head. It was found that the total moment of inertia ( $I_{total} = I_1 + I_2 + I_3$ ) of a 59 kg, 5'3" female standing upright with legs together and arms by the side is  $0.812kg * m^2$ . For this same subject with the left leg held out at an approximate 30 degree angle in a plane coplanar with the other leg,  $I_{total} = 1.0049kg*m^2$ , and with the right leg held out at an approximate 30 degree angle,  $I_{total} = 1.1987kg * m^2$ .

The new mathematical equations currently constrain moment of inertia values, I, and stiffness coefficients, K, to be positive values and allows the damping coefficient, B, to span all real values. Rather than there be one I, B, and K value for the entire pivot turn, the new model assumes that I, B, and K vary throughout and evaluates new I, B, and K values for each time segment throughout the pivot turn. Also, in the new approach the I of the head and stance leg are assumed to be constant and that of the torso, I, varies with time.

A pivot turn simulation has been constructed from this new model. The simulation is run on knowledge of obtained torque values and obtained moment of inertia values.

## 2. INTRODUCTION

This study is a continuation of a larger, ongoing project of Dr. Vijay Kumar and Dr. David Solomon of the Vestibular Ocular Motor Research Laboratory. The final goal of this research project is to model a pivot turn (foot driven gaze shift) through analysis of the dynamics involved in a pivot turn. Via data collected using force plates, an OPTOTRAK, and torsion pendulum, it is hoped that this analysis can be made. This collected data provides values for the ground reaction force acting on the foot, head position, pelvis position, thigh position, and foot position throughout five second time spans. From this data, theoretically, it is possible to determine the body moment of inertia (I), the ankle stiffness coefficient (B), and the ankle damping coefficient (K). These values will be crucial in understanding human movement.

### 3. BACKGROUND

**3.1. Motion Control.** When a person performs a movement, s/he maintains balance by achieving a proper body alignment, otherwise known as posture. Balance is a term used to describe the dynamic movement the body follows to prevent falling. To avoid a fall it is necessary to maintain the body axis along the resultant gravitational axis and properly oriented in space.

A person is able to control movement through three sensory systems: vision, the somatosensory system, and the vestibular system (Figure 1). The visual system permits locomotion with visual imaging of a stationary or moving target by creating an internal representation of the orientation of the object in space. The somatosensory system senses, via receptors in muscle and skin, the location and velocity of all body segments and their contact with external objects in order to guide directed movement. The vestibular system creates balance by sensing the linear and angular accelerations of the head in space. The information from the three systems is sent to the brain and central nervous system (CNS) integration occurs. The CNS sends a motor command to the body causing it to adjust. This body adjustment occurs, feedback is provided on the new body position in space, and this dynamic system is repeated to maintain balance.

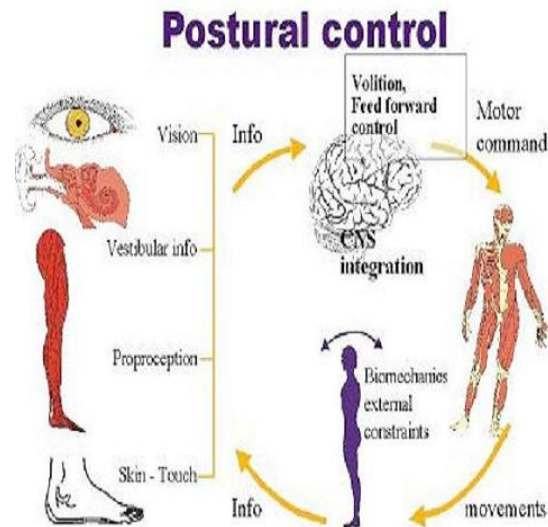


FIGURE 1. Postural Control  
Systems and Methods used for Balance and Postural Control

3.1.1. *Somatosensory System.* The somatosensory system is comprised of three modalities:

- Discriminative Touch: touch, pressure, and vibration perception
- Pain and Temperature: includes itch and tickle
- Proprioception: receptors that note activity occurring below the body surface such as muscle stretch, position, and tendon tension

The proprioception modality supplies constant feedback to the brain of joint position and muscle tension in the body and is important to this research. Proprioception controls the posture and movement of body parts by creating an internal representation of the body from stimuli responses in muscle spindles, Golgi tendon organs, and joint capsule receptors. This internal representation of the body is analyzed and motor commands are sent throughout the body to ensure that motor activities occur in a coordinated pattern.

Muscle spindles are small, encapsulated sensory receptors located in the fleshy region of muscles. Their purpose is to signal changes in the length of the muscle by evaluating the change in the angle of the joints that the muscle crosses. This, in turn, aids the central nervous system to sense relative locations of the body segments.

The golgi tendon organs are sensory receptors located at the junctions between muscle fibers and tendons. They contain sensory receptors that signal changes that occur in the muscle tension. The average level of activity of tendon organs in a muscle provides a reliable measure of the total force used in contracting muscle.

3.1.2. *Vestibular System.* The fovea is the section of the eye that maintains a clear image of an object. This clear image cannot be achieved by the visual system (VS) because the VS acts too slowly to process the movement of the head and allow focus to be maintained on an image. Thus, the nervous system relies on the vestibular system for the purpose of detecting head motion. The fovea is able to hold the image on the retina because appropriate information is sent to the about brain motion. Then an appropriate command is sent to the extra ocular muscles which rotate the eye (vestibulo-ocular reflex) which, in turn, holds the image on the fovea as the head rotates. Vestibulospinal mechanism also uses this sensory information to control antigravity and axial muscles in order to maintain equilibrium during static balance and dynamic behaviors such as locomotion and turning.

The vestibular system measures linear and angular acceleration of the head using five sensory organs in the inner ear (the membranous or vestibular labyrinth). From the sensory organs located in the inner ear, two different vestibulo-ocular reflexes occur:

- Rotational Vestibulo-ocular Reflex: Acts in response to a head angular acceleration and receives its input from the semicircular canals
- Translational Vestibulo-ocular Reflex: Acts in response to a linear head movement and gravity

Angular and linear acceleration of the head causes a shift in the positioning of filament bundles attached to hair cells in the vestibular labyrinth. This shift causes a change in the neurotransmitter release pattern of cells located in the membrane potential and transmitter which then causes a change in the discharge patterns of the vestibular neurons that innervate them. Vestibular neurons transmit the head velocity and acceleration signals to the vestibular nuclei in the brain stem, which aids in our ability to maintain balance and to perceive space. These signals generate compensatory eye movements in the opposite direction, allowing one to maintain a fixed gaze on an object while the head is in motion. These compensatory eye movements are known as the vestibular ocular reflex (VOR).

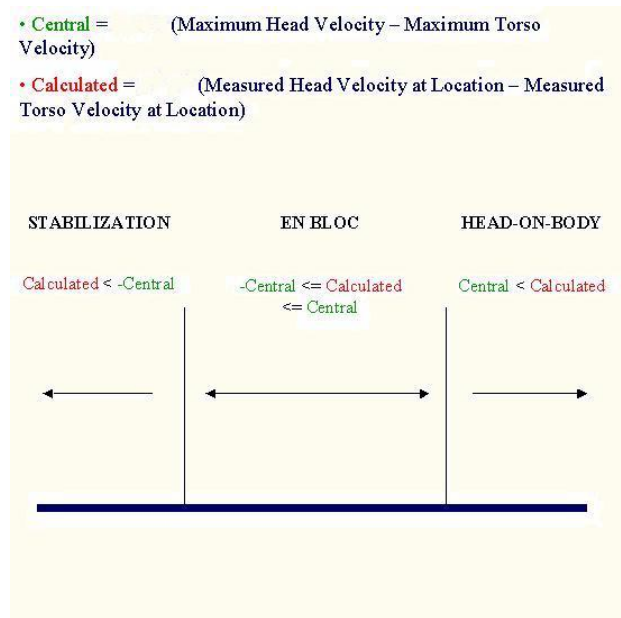


FIGURE 2. Stabilization, En bloc, and Head-on-Body Techniques  
Criteria used to Delineate Between Stabilization, En Bloc, and  
Head-on-Body Movement Techniques

3.1.3. *Movement Methods.* When performing a pivot turn, the body can move according to three methods:

- En bloc: The entire body moves as one unit, in which there is no significant rotation of body segments relative to one another
- Stabilization: Body segments move independently so that each segment aligns itself with the rest of the body
- Head-on-body: The head moves at a velocity much larger than the torso

Stabilization is when the difference between the measured head velocity and the measured torso velocity is less than the negative value of the difference between the maximum head velocity and the maximum torso velocity. En bloc is when the absolute value of the measured difference is less than the absolute value of the maximum difference. Head-on-body is when the measured difference is greater than the maximum difference. Figure 2 describes this criteria under which en bloc, head-on-body, and stabilization rotational methods are distinguished for this study.

3.2. **Mathematical Theory.** With the obtained dynamics and kinematics of a pivot turn, the understanding of human movement can be

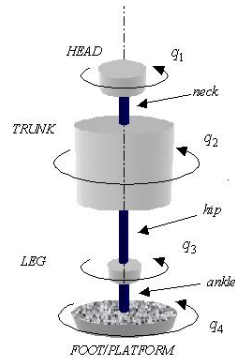


FIGURE 3. One Legged Model

greatly improved. To describe the kinematics involved in a pivot turn, it is necessary to know the moment of inertia of the body sections, the joints' effective stiffness coefficients, and the joints' effective damping coefficients. Throughout the upcoming analysis, all mathematical calculations follow the right hand rule convention.

The previous adopted model consisted of the following:

and is described by equation:

$$I_1\ddot{q}_1 + I_2\ddot{q}_2 + I_3\ddot{q}_3 + B_3\dot{\theta}_3 + K_3\theta_3 = \tau_3$$

The derivation of this equation will be provided in the following section. For the current pivot turn analysis, I have adopted a new three segment model of the human body. This is shown in figure 4. All further analysis refers to this improved figure.

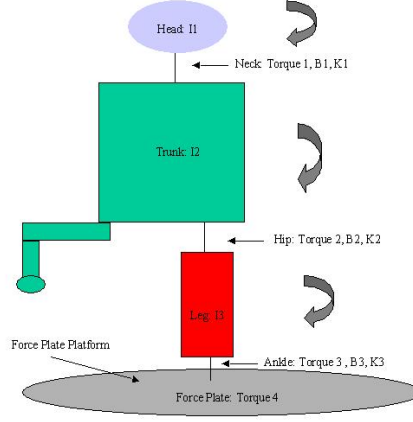


FIGURE 4. Mathematical Model

3.2.1. *OPTOTRAK and Force Plate Analysis.* The equations of motion for a pivot turn are:

$$\begin{aligned}
 (1) \quad & I_1 \ddot{q}_1 + B_1 \dot{\theta}_1 + K_1 \theta_1 = \tau_1 \\
 (2) \quad & I_2 \ddot{q}_2 + B_2 \dot{\theta}_2 + K_2 \theta_2 - B_1 \dot{\theta}_1 - K_1 \theta_1 = \tau_2 - \tau_1 \\
 (3) \quad & I_3 \ddot{q}_3 + B_3 \dot{\theta}_3 + K_3 \theta_3 - B_2 \dot{\theta}_2 - K_2 \theta_2 = \tau_3 - \tau_2
 \end{aligned}$$

where the constants  $K_i$  and  $B_i$  are the effective stiffness and damping coefficients across the  $i$ th joint, respectively,  $\tau_i$  is the  $i$ th joint torque,  $\theta_i = q_i - q_{i+1}$  is the  $i$ th joint angle,  $I_i$  is the moment of inertia for the  $i$ th body segment,  $\ddot{q}_i$ , is the angular acceleration across the  $i$ th joint angle,  $\dot{\theta}_i$  is the angular velocity across the  $i$ th joint angle, and  $\theta_i$  is the position of the  $i$ th joint.

Simplifying equations 1-3 results in the following:

$$(4) \quad I_1 \ddot{q}_1 + I_2 \ddot{q}_2 + I_3 \ddot{q}_3 + B_3 \dot{\theta}_3 + K_3 \theta_3 = \tau_3$$

Applying the following assumptions:

- $I_{trunk} = I_{wholebody} - I_{head} - I_{leg1}$
- $I_{trunk} = I_{pelvis} + I_{leg2}$
- $I_{head} = constant$
- $I_{leg1} = constant$

along with a bias of 100 to  $B_3$ , and simplifying gives the following:

(5)

$$I_1\ddot{q}_1 + I_2\ddot{q}_2 + I_3\ddot{q}_3 + (\bar{B}_3 + 100)\dot{\theta}_3 + K_3\theta_3 = \tau_3 + 100\dot{\theta}_3$$

(6)

$$I_1\ddot{q}_1 + I_2\ddot{q}_2 + (I_{total} - I_1 - I_2)\ddot{q}_3 + (\bar{B}_3 + 100)\dot{\theta}_3 + K_3\theta_3 = \tau_3 + 100\dot{\theta}_3$$

(7)

$$I_1(\ddot{q}_1 - \ddot{q}_3) + I_2(\ddot{q}_2 - \ddot{q}_3) + I_{total}\ddot{q}_3 + (\bar{B}_3 + 100)\dot{\theta}_3 + K_3\theta_3 = \tau_3 + 100\dot{\theta}_3$$

(8)

$$I_2(\ddot{q}_2 - \ddot{q}_3) + (\bar{B}_3 + 100)\dot{\theta}_3 + K_3\theta_3 = \tau_3 + 100\dot{\theta}_3 - I_1(\ddot{q}_1 - \ddot{q}_3) - I_{total}\ddot{q}_3$$

where  $I_{wholebody} = 1.0049kg * m^2$  and  $I_{head} = 0.0148kg * m^2$  [5].

Equation 8 can be rewritten in matrix notation as follows:

(9)

$$\begin{bmatrix} (\ddot{q}_2^1 - \ddot{q}_3^1) & \dot{\theta}_3^1 & \theta_3^1 \\ (\ddot{q}_2^2 - \ddot{q}_3^2) & \dot{\theta}_3^2 & \theta_3^2 \\ (\ddot{q}_2^3 - \ddot{q}_3^3) & \dot{\theta}_3^3 & \theta_3^3 \\ \vdots & \vdots & \vdots \\ (\ddot{q}_2^n - \ddot{q}_3^n) & \dot{\theta}_3^n & \theta_3^n \end{bmatrix} * \begin{bmatrix} I_2 \\ B_3 \\ K_3 \end{bmatrix} = \begin{bmatrix} \tau_{fp}^1 + \dot{\theta}_{avel}^1 * 100 - (\ddot{q}_1^1 - \ddot{q}_3^1) * I_1 - \ddot{q}_3^1 * I_{total} \\ \tau_{fp}^2 + \dot{\theta}_{avel}^2 * 100 - (\ddot{q}_1^2 - \ddot{q}_3^2) * I_1 - \ddot{q}_3^2 * I_{total} \\ \tau_{fp}^3 + \dot{\theta}_{avel}^3 * 100 - (\ddot{q}_1^3 - \ddot{q}_3^3) * I_1 - \ddot{q}_3^3 * I_{total} \\ \vdots \\ \tau_{fp}^n + \dot{\theta}_{avel}^n * 100 - (\ddot{q}_1^n - \ddot{q}_3^n) * I_1 - \ddot{q}_3^n * I_{total} \end{bmatrix}$$

where  $B_3 = \bar{B}_3 + 100$ .

In all calculations, the right hand rule convention is used. From equations 9, we can solve for the unknown parameters: the moment of inertia of the trunk,  $I_2$ , the damping coefficient of the ankle,  $B_3$ , and the stiffness coefficient of the ankle,  $K_3$ .

For a body rotated about the central axis, the total body moment of inertia,  $I_{total}$ , can be determined using the equation of motion:

(10)

$$\tau = I_{total} * \alpha$$

where  $\tau$  is the torque measured about the center of pressure of the foot and  $\alpha$  is the angular acceleration of the body. Integrating equation 10 twice for a 360 degree provides an estimation as follows:

$$(11) \quad \int \int \tau = I_{total} * \int \int \alpha$$

$$(12) \quad \int \int \tau = I_{total} * \theta$$

$$(13) \quad \int \int \tau = I_{total} * 2\pi$$

$$(14) \quad I = \int \int \tau / 2\pi$$

3.2.2. *Torsion Pendulum Analysis.* In order to obtain accurate I, B, and K values, the moment of inertia, I, can be calculated using a torsion pendulum. The mathematical derivation is as follows:

$$(15) \quad I = K_T * (1/\omega_n)^2$$

where  $\omega_n$  is the natural frequency of oscillation and  $K_T$  is the torsional spring constant.

The total mass moment of inertia of the standing subject ( $I_s$ ) is the difference between the I values determined with both the platform and subject, ( $I_{s+p}$ ), and with the platform alone, ( $I_p$ ),

$$(16) \quad I_s = I_{s+p} - I_p.$$

Using a torsion pendulum with two linear springs of spring stiffness coefficient,  $K_L = 254N/m$ , the following equation applies:

$$(17) \quad \tau = (F_1 - F_2) * R$$

$$(18) \quad = [(F_0 + K_L R \tan(\theta)) - (F_0 - K_L R \tan(\theta))] R$$

$$(19) \quad = 2K_L R^2 \tan(\theta)$$

where  $\tau$  is the applied torque on the platform, R is the radius of the platform, and  $F_0$  is the baseline tension of the spring before the disc is displaced. The torsional stiffness spring constant ( $K_T$ ) is related to torque as follows:

$$(20) \quad K_T = \tau / \theta$$

Substituting equation 20 into equation 19, we get:

$$(21) \quad K_T = 2K_L R^2 \tan(\theta) / \theta$$



FIGURE 5. OPTOTRAK and Force Plate

For the values of  $\theta$  use here,  $\theta = \tan(\theta)$ , so:

$$(22) \quad I_s = K_T(1/\omega_{s+p})^2 - K_T(1/\omega_P)^2$$

$$(23) \quad = 2K_L R^2 [1/(\omega_{s+p})^2 - 1/(\omega_p)^2]$$

#### 4. EXPERIMENTAL SETUP AND PROCEDURES

Several different apparatuses were used for this project's analysis. One is an OPTOTRAK and force plate set up, and the second is a torsion pendulum.

**4.1. OPTOTRAK and Force Plate.** Using the OPTOTRAK and force plate, as shown in figure 5, we were able to collect data of the force and torque the person applies to the ground and the person's body position with respect to time throughout a pivot turn. This data was transferred from ASCII format into Matlab to allow for data analysis.

IR markers were attached to the subject at eight locations: one on each foot, one on each thigh (directly above the knee), two at the pelvis (centered around the navel), and two on the forehead. The subject was asked to remove his/her shoes and to step on the force plate located at a distance of 8 feet from the OPTOTRAK. As the person stood on the force plate, the OPTOTRAK was aligned with the person until all of the markers could be viewed. Checking that all of the markers and the force and torque values were functioning and were being read properly, the data collection was initiated and the subject was asked to perform a right pivot turn. This procedure was also repeated for left pivot turns.

Next, data was collected to investigate the moment of inertia of the body throughout a pivot turn. The subject was instructed to hold his/her right leg to the front at a high (approximately 30 degrees), medium (approximately 15 degrees), and low angle (approximately 3 degrees) with respect to the center of the axis. The leg at 3 degrees with respect to the center axis served as the control.

The experiments were conducted as follows. For the control, the subject stood on one leg and did not move the adjacent leg. Thus, the person maintained balance on one leg as the data was collected. Next, the subject was instructed to stand on one leg with the other leg directly in front at an approximate 15 degree angle. After initiating the data collection, the subject was instructed to rotate his/her leg from the front to the side (a 90 degree rotation) and then back to the front in a smooth manner. Throughout the process the subject was to keep his/her foot and body facing forwards at all times (nonrotating ankle). This was repeated at approximately 30 degrees. Another experiment was conducted in which the subject allowed his/her foot and body to rotate the 90 degrees with the rest of the leg so as to be facing a 90 degree rotation with respect to the initial position (rotating ankle). This was then repeated in segments where the leg rotated from the front to the side, held in this position for 2 seconds, and then rotated from the side to the front for both a rotating and a nonrotating ankle at medium and high angles. Experiments were run on both the right and left leg.

Additionally, experiments were performed to calculate the subject's moment of inertia. The subject was instructed to make tiny steps turning about a single location with minimal deviation (preferably directly above this axis). The subject performed a 360 degree turn about this location with the arms by the side and then with the arms held out (perpendicular to the body and parallel to the shoulders). It is expected that the moment of inertia is larger when the arms are held out than when the arms are held by the side. The experiment was repeated with the subject rotating 720 degree with the arms by the side. It is expected that the moment of inertia for this experiment will give equivalent results to that of the subject performing a 360 degree turn with the arms by the side.

**4.2. Torsion Pendulum.** Following Albery's [1] methods to determine the moment of inertia of a seated human subject, an apparatus was constructed in Dr. Solomon's lab to measure the moment of inertia of a standing human subject about the z-axis of rotation. Contrary to Albery's apparatus, however, two linear springs are utilized as opposed

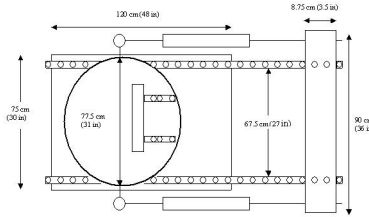


FIGURE 6. The Linear Pendulum Apparatus  
 An aerial-view blueprint of the Linear Pendulum Apparatus, showing the general layout along with important dimensions.

to a single torsional spring, still resulting in the oscillation of a base platform about a central axis while allowing for the necessary head-room to test a standing human subject on this apparatus within the laboratory.

The torsional pendulum system (figure 6), utilizing linear springs, is constructed upon a 120 x 75 cm (48 x 30 in) wooden plank with rectangular metal runners attached along each length of the plank. This base is bolted into the concrete floor of the laboratory using the runners. At one end of the base, a wooden circular disc with a diameter of 77.5 cm (31 in) was fixed to the base via a turntable to allow free rotation of the disc about its z-axis. At the opposite end of the base is an 8.75 x 8.75 x 90 cm (3.5 x 3.5 x 36 in) wooden block bolted along the top of the metal runners. Two identical springs are placed tangential to the circular disk so that an angle displacement causes the disk to rotate sinusoidally. Each spring is measured to have a linear spring constant of 254.01 N/m.

To maintain the body's center of mass about the central axis of rotation in the z-plane, subjects are fixed to an immobilization backboard extending from the central rotating platform. The backboard is stabilized to the platform through t-square plates bolted to the backboard and platform as well as trusses extending from the top of the backboard to the anterior base of the platform. Subjects are immobilized to the backboard using padded straps at the knees and waist (Figure 7).

Prior to data collection on the apparatus, subjects were required to remove their shoes. Subjects were then asked to stand on the circular platform with their left foot on the center of axis. This ensured that the center of mass was positioned directly above the coordinate system



FIGURE 7. Torsion Pendulum

A dual-spring torsional pendulum apparatus used to measure the Inertial Momentum in the Z-plane of standing subjects.

in line with the center of the rotating disk and that each trial was consistent with the others. Subjects were then fixed to the backboard with padded straps around the waist and knees. The right leg was held to the side at an approximate 30 degree angle by ducktaping the leg to the right struss. This ensured that the leg rotated at the same frequency as the rest of the body and torsion pendulum. Rate sensors were place against the backboard along the Z-axis of rotation by the planted foot and between the waist strap and the subject.

The platform was perturbed and allowed to oscillate sinusoidally until it came to rest. This was performed in both the clockwise and counterclockwise direction. This was repeated for the subject with the left leg held out. A LabView data collection program measured the velocity at 500 Hz for both rate sensors. This data was then evaluated to yield the frequency of oscillation for the sensors. This process was also repeated without the subject on the platform. The average frequency of oscillation without the subject on the platform was subtracted from the average frequency with the subject on the platform to yield the frequency of oscillation of the subject alone. Using the equations derived in section 3.2.2, the moment of inertia for the subject was calculated.

## 5. RESULTS

**5.1. OPTOTRAK and Force Plates.** All experiments conducted using the OPTOTRAK and force plates collected data at a 100 Hz

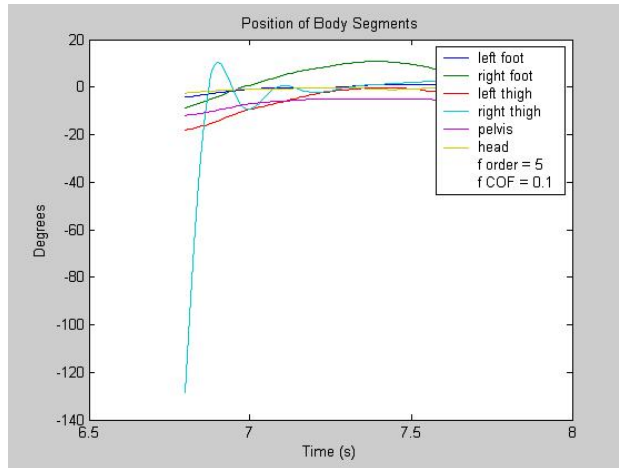


FIGURE 8. Position with respect to time

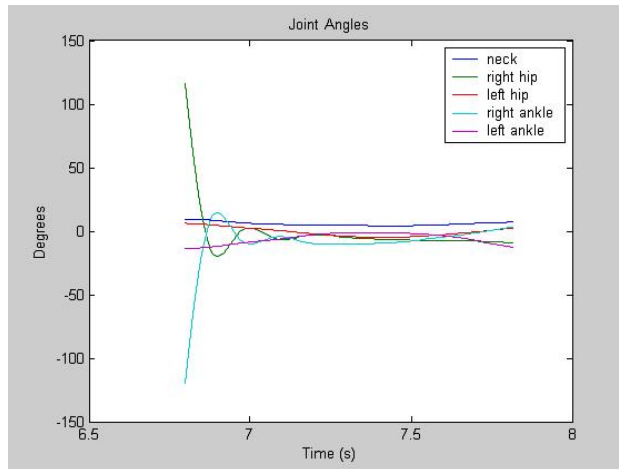


FIGURE 9. Joint segments with respect to time

sampling rate. All experimental data was gathered using a 5'3", 59 kg female subject.

Figures 8, 9, 10, and 11 respectively show the position of the body segments, joint segments, force and torque applied by the ankle to the ground, and the center of mass of the foot in the x- and y-coordinate directions with respect to time.

Figure 12 is a graph of the B and K values obtained through MATLAB analysis. As noted by the inconsistent values obtained, no confidence can be held in these results.

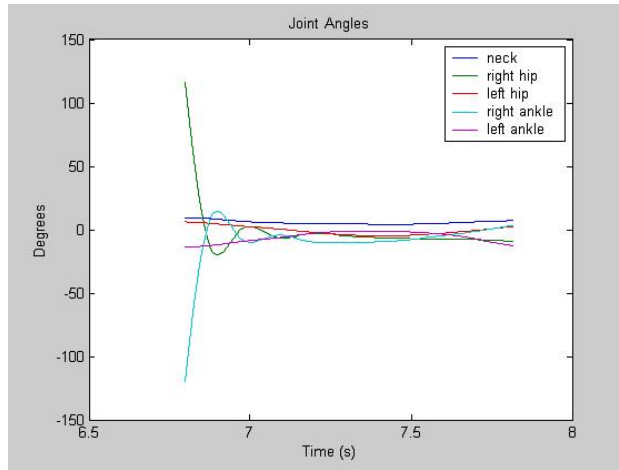


FIGURE 10. General features of pivot turn

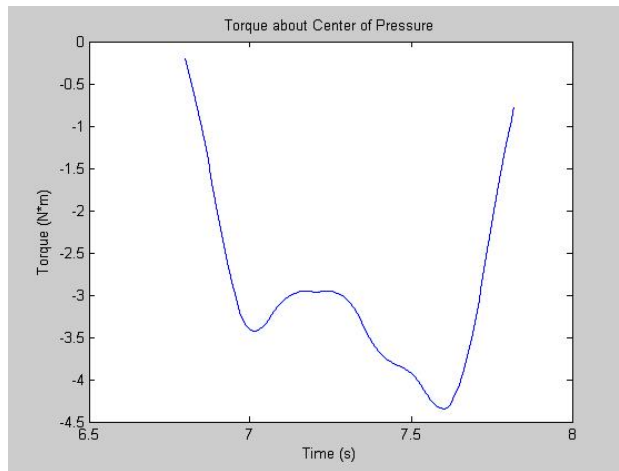


FIGURE 11. Torque applied to ground

Table 5.1 presents the MOI of a 59 kg, 5'3" female subject for 360 degree turns with the arms held both in and out, and for 720 degree turns with the arms held in. The data was collected at a 100 Hz sampling rate.

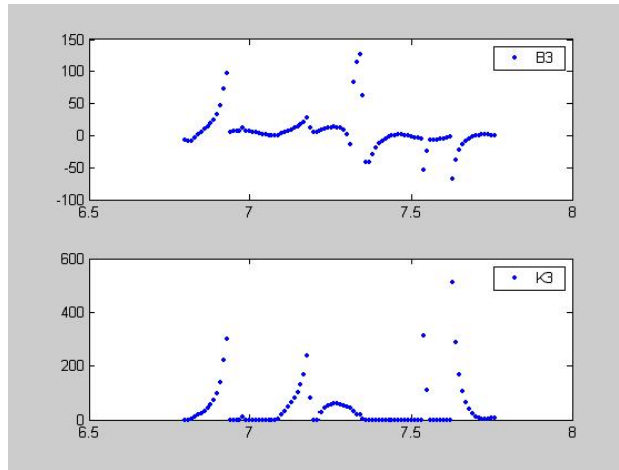


FIGURE 12. B and K Values

Trial Description	MOI ( $kg * m^2$ )
360 degree right turn, arms in	2.767
" " "	3.048
" " "	4.521
360 degree right turn, arms out	6.577
" " "	3.609
" " "	3.701
360 degree left turn, arms in	2.137
" " "	1.822
360 degree left turn, arms out	4.715
" " "	4.458
720 degree right turn, arms in	1.341
" " "	1.360
720 degree left turn, arms in	2.332
" " "	2.280

5.2. **Torsion Pendulum.** The moment of inertia was calculated from equation 23 and the data collected at a 500 scans/second sampling:

Trial Description	I ( $kg * m^2$ )
Person rotated counterclockwise	0.7657
Person rotated clockwise	0.6558
Person with Left Leg held out, rotated counterclockwise	1.0052
Person with Left Leg held out, rotated clockwise	1.1989
Person with Right Leg held out, rotated counterclockwise	1.0672
Person with Right Leg held out, rotated clockwise	1.0052

5.3. **Simulation.** A simulation was created to simulate the turning portion of the pivot turn. The moment of inertias calculated in table 5.2, along with the assumption that the mass ratios of the body are 15.7% for the leg, 75.9% for the trunk, and 8.4% for the neck. This along with the following measurements of the subject (measurements made for model are constructed in accordance with the model in figure 4) provided the following data:

Body Segment	Width (m), x-axis	Height (m), y-axis	Length (m), z-axis
Grounded Leg	0.1	0.8	0.15
Pivoting Leg	0.1	0.8	0.15
Trunk	0.41	0.6	0.15
Head	0.2	0.2	0.15

Body Segment	Mass (kg)	I ( $kg * m^2$ )		
Grounded Leg	9.263	0.511394792	0	0
		0	0.025087292	0
		0	0	0.501745833
Pivoting Leg	9.263	0.511394792	0	0
		0	0.025087292	0
		0	0	0.501745833
Trunk	35.518	1.13213625	0	0
		0	0.564144233	0
		0	0	1.563087983
Head	4.956	0.025813	0	0
		0	0.018585	0
		0	0	0.025813

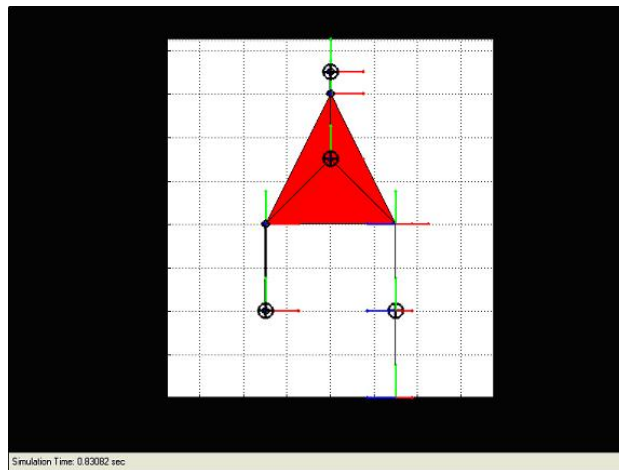


FIGURE 13. Simulated pivot turn at an initial time

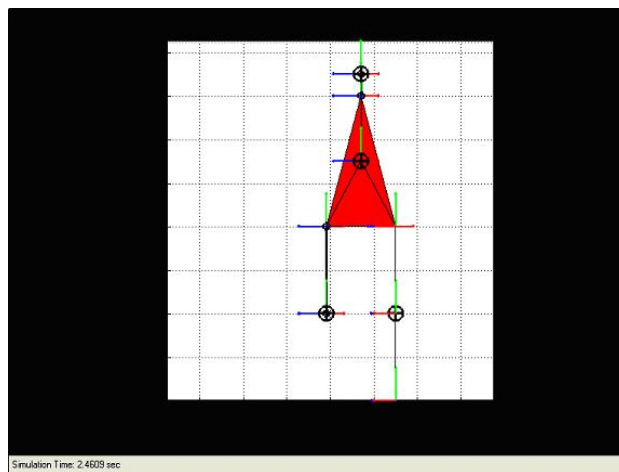


FIGURE 14. Simulated pivot turn at a middle time

This information, along with figure 11, was implemented into the simulated pivot turn model. Figures 13 and 14 are two frames from this avi clip:

## 6. DISCUSSION

The goal of this project is to improve the human model used for analyzing a pivot turn. The previous one-legged model did not provide plausible data, so I have created a new model. This model (Figure 4) currently describes  $I_1$  as the leg in contact with the ground,  $I_2$  as the pelvic section including the leg held out to the side, and  $I_3$  as the head.

This is more realistic because this new model considers the fact that the pivot turn begins on two legs, spins on one leg, and ends up on two legs again. Also it allows the moment of inertia of the leg to vary with time.

The mathematical equation has also been improved from the previously used one. The current analysis is noted in the mathematical theory section 3.2. In previous analysis, all three segments were given the freedom to be both positive and negative values and each segment's  $I$  varied with time. In this analysis,  $I$  and  $K$  solutions are constrained to be positive values and  $B$  spans positive and negative values. Also, in the new approach the  $I$  of the head and standing leg are constants and that of the torso, varies with time. This is because we're assuming that only the trunk section's  $I$  has a possibility to change, as noted by the leg raising and lowering. The change of the moment of inertia due to the leaning of the body is assumed to be insignificant and is not accounted for in this model. Another improvement to the model is that the  $I$ ,  $B$ , and  $K$  values will vary throughout the pivot turn, whereas in the previous analysis it was assumed that there is only one  $I$ ,  $B$ , and  $K$  value for the entire pivot turn. This should be valid because the dynamics should be changing during different phases of the pivot turn.

One topic of uncertainty should be pointed out. This is how many data points should we use to derive the  $I$ ,  $B$ , and  $K$  values. It should be noted that taking a greater number of data points will create greater correspondance between values. However, this may be misleading because it does force there to be significance between data points which either wise may not be there. In performing the MATLAB analysis, this is one issue that has been and will be further investigated.

I went about the pivot turn analysis by trying to break the pivot turn into its individual pieces. Due to there being an initial torque offset when standing in a double leg stance, I collected data for subjects standing on and beginning the pivot turn from one leg. The torque values for a right pivot turn with the leg held at a 30 degree angle can be viewed in figure 11. This experiment did not give possible  $I$ ,  $B$ , and  $K$  values so I broke the problem down even further. I solved for one of the values, the moment of the inertia,  $I$ . Thus, I determined the body's  $I$  and implemented this value into the code so that  $B$  and  $K$  would be the only free variables. Unfortunately with this improvement, the  $B$  and  $K$  values still remained illogical. It may be due to an inaccurate method of generating the pivot turn model. Also error may arise due to the noise which is amplified when taking the second derivative for the analysis.

The determination of the moment of inertia using the OPTOTRAK and force plates also proved unsuccessful. Although this method of analysis worked for Albery [1], my method of analysis did not work. It may be because I did not take the derivatives of the position markers with respect to time but rather I took the double integral of the torque with respect to time and applied the known angle into equation 14. For further experiments, I should take the derivatives of the rate sensor position data to calculate the moment of inertia.

Using the torsion pendulum and MATLAB, I was able to calculate the moment of inertia of the body. The calculation of moment of inertia is dependent on two factors: the spring constant and the frequency of oscillation, as noted in equation 15. I have calculated the moment of inertia of the body as a whole for the position held throughout a pivot turn (leg outstretched and body slightly leaning) and for the initial stance on two feet. For a 5'3", 59 kg subject, the moment of inertia in the pivot turn position ranges from  $1.0052 \text{ kg} * \text{m}^2$  to  $1.1989 \text{ kg} * \text{m}^2$ , and in the normal stance ranges from  $0.6558 \text{ kg} * \text{m}^2$  to  $0.7657 \text{ kg} * \text{m}^2$ .

Incorporating all of these advances of the pivot turn model, I have created a pivot turn simulation. Although the B and K values are not the actual values that occur in a pivot turn, the motion of the pivot turn appears similar to that as performed in the experiment with the OPTOTRAK and force plates. The simulation is built from the dimensions and inertia matrices as given in tables 5.3 and 5.3. It is assumed that the mass is evenly distributed throughout each body segment. The simulation, which is presented in figures 13 and 14, is actuated by a joint actuator with a torque at the ankle joint similar to that shown in figure 11. This joint actuator is what produces the pivot turn motion in the simulation.

## 7. CONCLUSIONS AND FUTURE WORK

I have presented a dynamic simulation of a pivot turn based on calculated I values. These values were determined from my results on the torsion pendulum. Although this model does not provide actual known dynamic values, it is based on known I results and is a step forward to a possible theoretical model.

The new model continues to describe the human body as a three segment system consisting of three joints. One segment is the leg in contact with the ground, the second segment is the pelvic section plus the leg which is held out to the side throughout the pivot turn, and the third segment is the head. This model describes the moment of inertia of the body to be different depending whether the person is tilted (the

middle of the pivot turn) or standing straight up with legs together (the start and finish of the the pivot turn).

The next step is to calculate B and K values and to input these into the simulated model. With further analysis for the B and K values, this simulation can be once again revised and updated. The model can be used to check the validity of the values determined. If these values produce a pivot turn similar simulation to that of a real pivot turn, I can try to input one of these values into the MATLAB code and try to obtain the unknown value, thus verifying the accuracy of this model. I also may choose to use an EMG to see if the muscle activity coincides with these B and K values. This may allow for a more biological understanding of the pivot turn.

Results from these experiments demonstrate the importance of lower extremity somatosensory information on head motor control, an example of bottom-up-processing. It is hoped that with an increased understanding of the lower extremity somatosensory information, balance disorders can be better understood and treated.

## 8. ACKNOWLEDGEMENTS

I would like to thank Dr. David Solomon, Professor Vijay Kumar, and Patrick Yannul for walking me through this research.

## REFERENCES

- [1] Albery, Christopher M., Capt. Rebecca B. Shultz, and Valerie S. Bjorn. "Measurement of Whole-Body Human Centers of Gravity and Moments of Inertia."
- [2] Kandel, Eric R., James H. Shwartz, and Thomas M. Jessel. *Principles of Neural Science* 4<sup>th</sup> ed. New York: McGraw Hill, 2000.
- [3] Keshner, E.A., and B. W. Peterson. "Mechanisms Controlling Human Head Stabilization. Head-Neck Dynamics During Random Rotations in the Horizontal Plane." *The American Physiological Society* June 1995: 2, 293-301.
- [4] Molavi, Diana Weedman. *Basic Somatosensory Pathway*. The Washington University School of Medicine. 28 May 2003 <<http://thalamus.wustl.edu/course/bassens.html>>.
- [5] Peng, G. C. Y., T. C. Hain, and B. W. Peterson. "A dynamical model for reflex activated head movements in the horizontal plane." *Biological Cybernetics* 75 1996: 309-319.
- [6] Shepard, Neil T, and David Solomon. "Functional Operation of the Balance System in Daily Activities." *Otolaryngologic Clinics of North America* June 2000: 455-69.
- [7] Winter, D. A. "Human balance and posture control during standing and walking." *Gait & Posture* December 1995: 193-214.
- [8] Winter, D. A., Aftab E. Patla, Shirley Rietdyk, and Milad G. Ishac. "Ankle Muscle Stiffness in the Control of Balance During Quiet Standing." *The American Physiological Society* 19 February 2001: 2630-2633.

NETTA GURARI ADVISORS: PROFESSOR VIJAY KUMAR DR. DAVID SOLOMON

Appendix